

Multifractal description of fracture morphology. Full 3D analysis of a fracture surface

SEBASTIAN STACH^{1*}, JERZY CYBO¹, JAN CWAJNA², STANISŁAW ROSKOSZ²

¹Department of Materials Science, Silesian University, ul. Snieżna 2, 41-200 Sosnowiec, Poland

²Department of Materials Science, Silesian University of Technology,
ul. Krasińskiego 8, 40-019 Katowice, Poland

Experimental verification of the theoretical methodology for describing a material's fracture morphology using multifractal analysis of a stereometrically examined surface (full 3D analysis) is presented. A high effectiveness of a multifractal analysis has been shown for a diversified multifractal spectrum width and for a quantitative description of overlaps. The values obtained are very similar to those obtained by the quasi 3D method [6] as well as by conventional analysis, that is analysis of the profile images obtained from transverse microsections. The method presented, however, is the least time-consuming, the cheapest and seems to be the most objective for fracture morphology analyses.

Key words: *fracture; surface; stereometry; overlaps; profile; multifractal; spectrum width*

1. Introduction

One of important tasks in material engineering is optimization of the material's properties, inter alia crack resistance [1]. Assuming that a fractal characterization of a profile line reveals more about the crack surface microgeometry and complexity of the crack path, a concept has been proposed for considering the problem of profile development in terms of a multifractal analysis [2–5]. The multifractal spectrum parameters should be closely related to the degree of profile development.

A completely new methodology of stereometric research of a very large number of mutually perpendicular profiles (quasi-3D method) which form a spatial image of the micro-geometry of a fracture surface has been applied [6]. The measurements were made using a Taylor-Hobson's TalySurf Series 2 profilographometer. For each perpendicular direction of a profile's position, a multifractal analysis was performed. The

*Corresponding author, e-mail: sstach@us.edu.pl

obtained spectrum widths were averaged and the percentage share of overlaps was calculated in accordance with the principles provided in [6–8]. The analyzed materials were seven grades of sintered carbide, WC-Co, of a two-phase structure having different tungsten carbide grain size and volume fractions of the cobalt phase.

The present paper aims at providing an unquestionably simplified research methodology. The idea of the full 3D method is to consider globally a surface measured with a profilographometer, without the need to analyse individual profiles [6]. It is expected that after applying relevant multifractal procedures and determining the width of a spectrum, the percentage share of overlaps should be determined more precisely and at much lower cost and labour usage than in the case with earlier presented methods.

2. Research tools

The research was undertaken with the tools and material described in [6]. The analysis of the fracture's stereometric files was based on an original algorithm consisting of fractal scaling (in many approximation steps) of the surface measured with a profilographometer followed by the calculation of Euclidean distances between the measuring points (for a given scale and box). The measurements of the surface were made with the greatest possible accuracy in order to meet the criterion in which the “box” size in the box-counting method is approaching zero (Fig. 1).

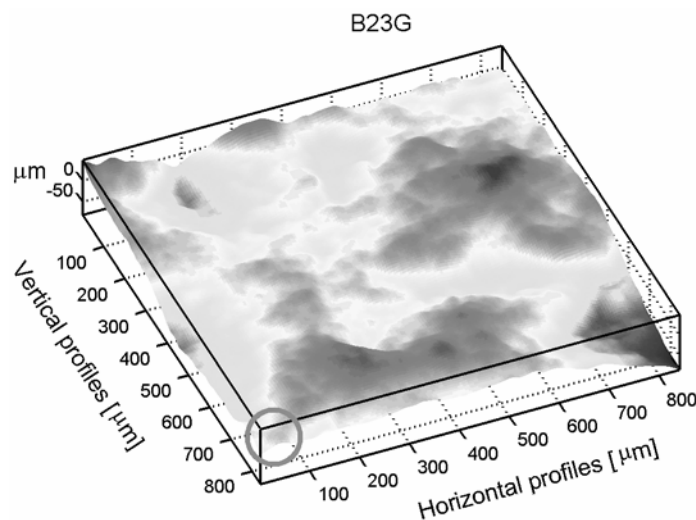


Fig. 1. Isometric view of a surface with a marked small area whose enlarged image is shown in Fig. 2

Next, changing the size of boxes was simulated by changing the measuring density. By selecting every 1st, 2nd, 3rd, 4th, 5th, 6th, 7th, 8th, 10th, 12th, 14th, 15th,

20th, 21st, 24th, 28th, 30th, 35th, 40th, 42nd, 56th, 60th, 70th, 84th, 105th, 120th, 140th, 168th, 210th, 280th and 420th measuring point from the entire surface measured (Fig. 1) for the analysis, 31 scalings of the surface were obtained (Fig. 2) which approximate to the real appearance of the surface when the distance between the measuring points decreases.

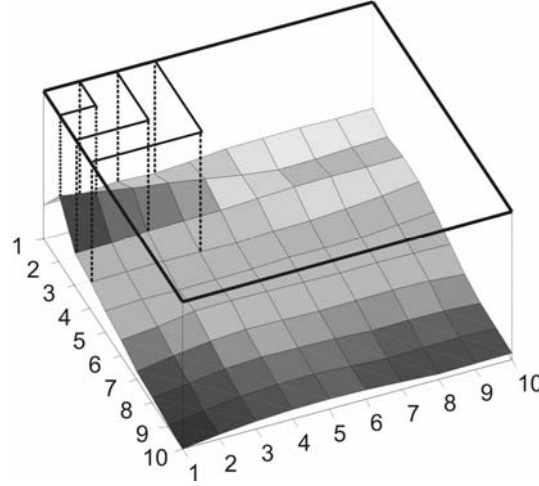


Fig. 2. Three exemplary (every 1, 2, 3 measuring points) scalings of the surface measured

For the scaling matrices obtained (Fig. 3), an algorithm was applied consisting of calculating Euclidean distances (Fig. 4) between the closest neighbouring measuring points in each scaling step (1):

$$\begin{bmatrix} \text{Euc_dist}_{a-b} = [\delta^2 + (h_{ai} - h_{bi})^2]^{1/2} \\ \text{Euc_dist}_{b-c} = [\delta^2 + (h_{bi} - h_{ci})^2]^{1/2} \\ \text{Euc_dist}_{c-d} = [\delta^2 + (h_{ci} - h_{di})^2]^{1/2} \\ \text{Euc_dist}_{d-a} = [\delta^2 + (h_{di} - h_{ai})^2]^{1/2} \end{bmatrix} \quad (1)$$

Next, for each of the measuring fields the maximum value was selected from 4 Euclidean distances for a given measuring field (2):

$$A_i(\delta) = \max \begin{bmatrix} \text{Euc_dist}_{a-b} & \text{Euc_dist}_{b-c} \\ \text{Euc_dist}_{c-d} & \text{Euc_dist}_{d-a} \end{bmatrix} \quad (2)$$

The values of maximum Euclidean distances were recorded in separate matrices (3) for each scale:

$$\begin{bmatrix}
 A_{w,k \quad w,k}(\delta) & \cdots & \cdots & A_{1,840 \quad 1,841}(\delta) \\
 & & & 2,840 \quad 2,841 \\
 & \cdots & & \cdots \\
 & \cdots & & \cdots \\
 & \cdots & & \cdots \\
 A_{5,1 \quad 5,2}(\delta) & & & \cdots \\
 & 6,1 \quad 6,2 & & \\
 & \cdots & & \cdots \\
 A_{840,1 \quad 840,2}(\delta) & \cdots & \cdots & A_i(\delta) \\
 & 841,1 \quad 841,2 & &
 \end{bmatrix} \quad (3)$$

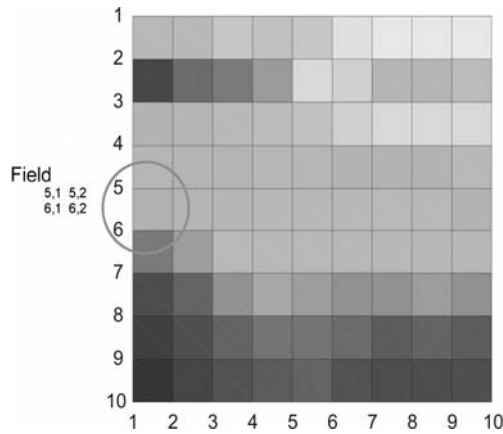


Fig. 3. Exemplary matrix of 9 per 9 measuring fields with a marked single field and its coordinates

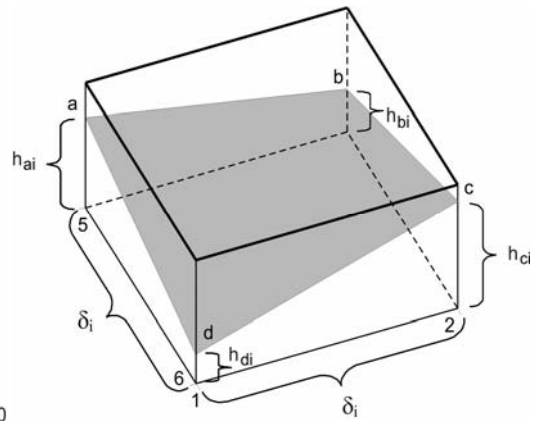


Fig. 4. Enlarged, isometric view of an exemplary measuring field with marked characteristic points

The probability was estimated (4) of the occurrence of each of the maximum Euclidean distance values:

$$P_i(\delta) = \frac{A_i(\delta)}{A_Y(\delta)} \quad (4)$$

As a result, 31 matrices of multifractal measurements were obtained for each specimen (5), which were then subjected to analysis in accordance with the principles provided in [4–9]:

$$\begin{bmatrix}
 P_{w,k \quad w,k}(\delta) & \cdots & \cdots & P_{1,840 \quad 1,841}(\delta) \\
 w,k \quad w,k & & & 2,840 \quad 2,841 \\
 \cdots & & & \cdots \\
 \cdots & & & \cdots \\
 \cdots & & & \cdots \\
 P_{5,1 \quad 5,2}(\delta) & & & \cdots \\
 6,1 \quad 6,2 & & & \\
 \cdots & & & \cdots \\
 P_{840,1 \quad 840,2}(\delta) & \cdots & \cdots & P_i(\delta) \\
 841,1 \quad 841,2 & & &
 \end{bmatrix} \quad (5)$$

3. Results and discussion of the multifractal analysis

The outcomes of these procedures were seven multifractal spectra (Fig. 5), the characteristic values of which are shown in Table 1.

The most important parameter from the point of view of the method described, is the width of arm's spacing of the multifractal spectrum whose interpretation has been provided in papers [6–9].

A transition from the quasi-3D analysis [6] to this full 3D analysis implies changes of the capacitive dimension D_0 from the value of 1 to 2. This is caused by the analysis of the two-dimensional matrix of Euclidean distances as opposed to the quasi-3D analysis where a one-dimensional list is subjected to an analysis. The multifractal spectrum widths are, in both cases, in full correlation, which enables a suitable conversion of the spectrum values based on a regression equation (the correlation diagram of both methods). The results are presented in Table 2.

On the basis of the converted widths of spectra, following the idea presented in [8], the percentage share of overlaps was estimated. The results are provided in Table 3.

The calculated percentage share of overlaps shows very high convergence with the values obtained both using the quasi 3D analysis and the conventional analysis based on quantitative fractography.

Although both methods (3D and quasi-3D) are similar, in the case of the former, slight differences in the estimation of the overlap's percentage share can be observed. This is caused by the selection of the maximum value from the four values calculated for each of the measuring fields.

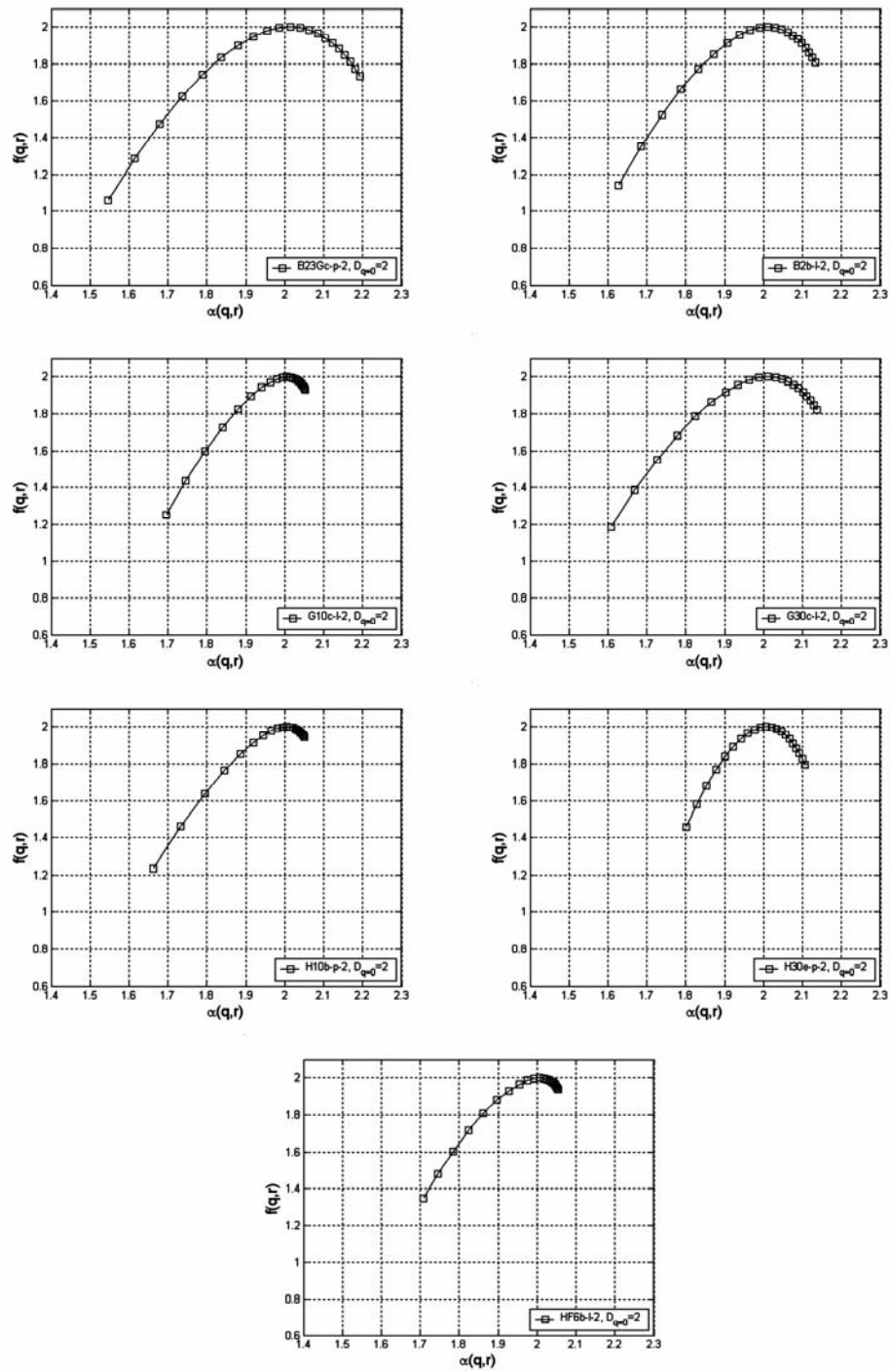


Fig. 5. Results of multifractal analysis for seven sintered carbide grades

Table 1. Characteristic values of multifractal spectra

Material	D_0	α_0	D_1	α_1	D_2	α_2	α_{\min}	α_{\max}	Width
B23G	2.0000	2.0140	1.9855	1.9855	1.9786	1.9539	2.1938	1.5454	0.6483
B2b	2.0000	2.0105	1.9890	1.9890	1.9819	1.9647	2.1321	1.6275	0.5046
G10	2.0000	2.0054	1.9941	1.9941	1.9895	1.9801	2.0525	1.6955	0.3571
G30	2.0000	2.0109	1.9886	1.9886	1.9832	1.9634	2.1364	1.6075	0.5289
H10	2.0000	2.0051	1.9946	1.9946	1.9916	1.9816	2.0496	1.6614	0.3882
H30	2.0000	2.0073	1.9926	1.9926	1.9852	1.9767	2.1058	1.8013	0.3045
HF6	2.0000	2.0065	1.9929	1.9929	1.9876	1.9757	2.0545	1.7074	0.3471

Table 2. Comparison of the values of multifractal spectrum widths obtained by two methods

Material	Multifractal spectrum width (quasi 3D analysis)	Multifractal spectrum width (3D analysis)	Multifractal spectrum width (3D analysis) (calculated)
B23G	0.2963	0.6483	0.3039
B2	0.2219	0.5046	0.2398
G10	0.1914	0.3571	0.1740
G30	0.2672	0.5289	0.2506
H10	0.1811	0.3882	0.1879
H30	0.1561	0.3045	0.1505
HF6	0.1622	0.3471	0.1695

Table 3. Comparison of the overlaps' percentage share values obtained by conventional method and by applying multifractal techniques

Material	Percentage share of overlaps (full 3D analysis)	Percentage share of overlaps (quasi 3D analysis)	Percentage share of overlaps (microscope)
B23G	10.35	9.90	11.40
B2	6.73	5.60	7.12
G10	3.01	3.84	3.31
G30	7.34	8.22	7.64
H10	3.79	3.24	4.70
H30	1.68	1.80	2.53
HF6	2.76	2.15	2.79

4. Conclusions

The study aimed at maximum simplification of the research methodology by reducing it to a stereometric measurement of the fracture surface and next, to a multifractal analysis of the file obtained. Eventually, spectrum widths were obtained which in an indirect way enable the estimation of the overlap's percentage share for the en-

tire surface (full 3D analysis). High conformity of this methodology with the quasi 3D method presented in [6] has been shown.

The new method is simple and is characterized by low costs and labour consumption, which together ensure high effectiveness. It allows the right diversity in the fractal characteristics of fracture surface measured with a profilographometer. The multifractal spectrum width changes proportionally to the surface development degree, thus constituting a quantitative characterization of the entire surface analyzed, not only of a single profile.

It should be noted that the presented solution has been verified for one material characterized by a specific type of cracking, i.e. WC-Co carbides. As far as other materials are concerned, similar investigations should be conducted. The conclusions presented corroborate the results obtained for the 34CrMo4 steel [9]. In the same paper, the possibility of using the same formula which allows conversion of the spectrum width into the percentage share of overlaps was identified. This, however, requires confirmation, based on other cases, to be obtained.

References

- [1] ROSKOSZ S., *Zastosowanie metod stereologicznych w ocenie dekohezji węglików spiekanych*, PhD Thesis, Silesian University of Technology, Katowice, 2000.
- [2] MANDELBROT B. B., *The fractal geometry of nature*, W. H. Freeman and Comp., New York, 2000.
- [3] FEDER J., *Fractals*, Plenum Press, New York, 1989.
- [4] XIE H. WANG J.-A. STEIN E., *Phys. Letters A*, 242 (1998), 41.
- [5] CHHABRA A., JENSEN R. V., *Phys. Rev. Lett.*, 62 (1989), 1327.
- [6] STACH S., CWAJNA J., ROSKOSZ S., CYBO J., *Mater. Sci.-Poland*, 23 (2005) 573.
- [7] STACH S., CYBO J., *Materials Characterization*, 51 (2003), 79.
- [8] STACH S., ROSKOSZ S., CYBO J., CWAJNA J., *Materials Characterization*, 51 (2003), 87.
- [9] STACH S., SOZAŃSKA M., CYBO J., CWAJNA J., *Acta Metallurgica Slovaca*, 10 (2004), 768.

Received 6 September 2004

Revised 5 January 2005